Biogeochemical and Isotopic Gradients in a BTEX/PAH Contaminant Plume: Model-Based Interpretation of a High-Resolution Field Data Set

ARTICLE *in* ENVIRONMENTAL SCIENCE AND TECHNOLOGY · NOVEMBER 2009

Impact Factor: 5.33 · DOI: 10.1021/es901142a · Source: PubMed

5 AUTHORS, INCLUDING:

Henning Prommer
University of Western Australia / CSIRO Lan…
112 PUBLICATIONS **1,884** CITATIONS
SEE PROFILE

Massimo Rolle
Technical University of Denmark
67 PUBLICATIONS **825** CITATIONS
SEE PROFILE

Christian Griebler
Helmholtz Zentrum München
80 PUBLICATIONS **2,223** CITATIONS
SEE PROFILE

Environ. Sci. Technol. **2009,** *43,* 8206–8212

Biogeochemical and Isotopic Gradients in a BTEX/PAH Contaminant Plume: Model-Based Interpretation of a High-Resolution Field Data Set

HENNING PROMMER,[†,‡] BETTINA ANNESER,[*,§,#] MASSIMO ROLLE,[∥] FLORIAN EINSIEDL,[⊥] AND CHRISTIAN GRIEBLER[§]

CSIRO Land and Water, Private Bag No. 5, Wembley WA 6913, Australia, School of Earth and Environment, University of Western Australia, Crawley, Western Australia, Helmholtz Zentrum München, Institute of Groundwater Ecology, Ingolstädter Landstr. 1, 85764 Neuherberg, Germany, Centre for Applied Geosciences, University of Tübingen, Sigwartstrasse 10, 72076 Tübingen, Germany, and Department of Environmental Engineering, Technical University of Denmark, 2800 Kgs. Lyngby, Denmark

Received April 15, 2009. Revised manuscript received September 3, 2009. Accepted September 3, 2009.

A high spatial resolution data set documenting carbon and sulfur isotope fractionation at a tar oil-contaminated, sulfate-reducing field site was analyzed with a reactive transport model. Within a comprehensive numerical model, the study links the distinctive observed isotope depth profiles with the degradation of various monoaromatic and polycyclic aromatic hydrocarbon compounds (BTEX/PAHs) under sulfate-reducing conditions. In the numerical model, microbial dynamics were simulated explicitly and isotope fractionation was directly linked to the differential microbial uptake of lighter and heavier carbon isotopes during microbial growth. Measured depth profiles from a multilevel sampling well with high spatial resolution served as key constraints for the parametrization of the model simulations. The results of the numerical simulations illustrate particularly well the evolution of the isotope signature of toluene, which is the most rapidly degrading compound and the most important reductant at the site. The resulting depth profiles at the observation well show distinct differences between the small isotopic enrichment in the contaminant plume core and the much stronger enrichment of up to 3.3‰ at the plume fringes.

Introduction

The fate of organic pollutants in groundwater systems is typically controlled by a combination of biochemical and physical processes. Oxidizable compounds such as aromatic hydrocarbons may be degraded by a combination of various redox reactions involving dissolved (oxygen, nitrate, sulfate) or mineral-form (e.g., iron/manganese oxides) electron acceptors. Earlier numerical studies (*1*), controlled laboratory-scale experiments (*2*−*5*) and field investigations (*6*−*8*) assumed or suggested that biochemical turnover rates may be particularly high at contaminant plume fringes where soluble electron donors and acceptors mix due to transverse hydrodynamic dispersion. This conceptual model implies the occurrence of steep geochemical gradients and the formation of narrow bioactive zones at locations where electron donors and electron acceptors overlap. Recent scenario-type numerical modeling of fringe-controlled degradation processes by van Breukelen and Prommer (*9*) indicated that the associated accelerated isotopic enrichment in fringe zones may also lead to the formation of distinct isotopic gradients across contaminant plumes. In the absence of adequately resolved spatial data such variations in lateral or, even more pronounced, in vertical directions were not recognized. As a consequence, such variations were ignored in the interpretation of carbon isotope data. However, Fischer et al. (*10*) recently presented detailed depth profiles of carbon and hydrogen isotopes for a degrading benzene plume. The vertical spacing of the monitoring ports of 0.5−1 m was sufficient to delineate the major concentration and isotope fractionation patterns of the 8 m thick plume. Based on the measured changes in the isotope ratio, the Rayleigh equation was applied to calculate the extent of biodegradation. Also recently, Anneser et al. (*11, 12*) developed and implemented high-resolution instrumentation (sampling port separation as small as 2.5 cm) for a BTEX/PAH contaminated, sulfate-reducing field site where the plume thickness was <1 m. This enabled an extremely detailed delineation of biogeochemical and isotopic gradients.

In this study we used this high resolution data set to evaluate whether our conceptual understanding of coupled transport, biogeochemical reactions and associated isotopic changes could be consistently explained within a quantitative framework. Therefore, we developed a numerical reactive transport model that integrated all major biogeochemical reactions hypothesized for the study site and used it to evaluate the process-based representation of microbially driven carbon ($\delta^{13}C$) and sulfur ($\delta^{34}S$) isotope enrichment.

Materials and Methods

Field Site. The study site is located at a former gasworks site in Düsseldorf-Flingern, Germany. The aquifer below the site received considerable input of mono- and polycyclic aromatic hydrocarbons (especially toluene and naphthalene) during the production of tar oil compounds from 1897 to 1967. The saturated zone is characterized by relatively homogeneous quaternary sediments exhibiting a mean hydraulic conductivity of 1×10^{-3} m s^{-1}. A layer of low permeable Tertiary fine sand confines the aquifer at the bottom. Groundwater flows from east to west along a hydraulic gradient of 0.006 at an estimated mean pore velocity of 1.5 m d^{-1} (*11, 12*).

Excavation of soil (>55 000 t) between 1995 and 1997 removed most of the tar oil from the unsaturated zone, but failed to completely remove the nonaqueous phase liquid (NAPL) contaminant from the saturated portion of the aquifer, especially where soils were covered by buildings. The remaining contaminants formed a plume of about 200 m length and 30 m width, consisting mainly of aromatic hydrocarbons, above all toluene, xylenes, and naphthalene. A network of several fully screened and multilevel sampling

* Corresponding author phone: +49-89-31873893; fax: +49-89-31873361; e-mail: bettina.ruth@helmholtz-muenchen.de.
† CSIRO Land and Water.
‡ University of Western Australia.
§ Institute of Groundwater Ecology.
∥ University of Tübingen.
⊥ Technical University of Denmark.
Current address: Helmholtz Zentrum München, Institute of Groundwater Ecology, Ingolstädter Landstrasse 1, D-85764 Neuherberg, Germany.

10.1021/es901142a CCC: $40.75
Published on Web 09/24/2009

wells was established in order to monitor the distribution of the contaminants (see Supporting Information (SI) Figure SI-1). In June 2005, a novel high spatial resolution multilevel well with vertical sampling intervals of 2.5−33 cm was installed in the centerline of the BTEX plume, approximately 15 m downstream of the presumed tar oil source. Simultaneous sampling of up to 32 filter ports at low pumping rates using protocols specifically tailored to the analysis of low sampling volumes allowed the identification of steep geochemical and isotopic gradients as well as various microbiological parameters. Compound-specific stable isotope analysis of aromatic hydrocarbons ($\delta^{13}C$) was performed using a Trace GC analyzer (Thermo Finnigan, San Jose, CA), which was coupled to an isotope ratio mass spectrometer (Thermo Finnigan MAT, Bremen, Germany). Upstream of the GC-IRMS system, a purge and trap concentrator (Tekmar LSC 3100) was connected to a liquid autosampler (Tekmar AQUAtek 70, Tekmar-Dohrmann, Mason, OH). Analytical measurements and calculations of the carbon isotope ratios were performed as described by Zwank et al. (*13*). More detailed information on the history and hydrology of the site as well as on sampling procedures is given elsewhere (*11, 12*). Protocols for the analysis of the stable isotope composition of groundwater sulfate ($\delta^{34}S$) and calculation of sulfate isotope ratios are reported in ref *11*.

Modeling Framework. The reactive multicomponent transport model PHT3D (*14*) was adopted to simulate biogeochemical and isotopic changes in a two-dimensional vertical transect along the contaminant plume's center axis. PHT3D has previously been used to simulate complex biogeochemical subsurface processes (e.g., refs *15−17)* and to model isotope fractionation associated with organic compound degradation (*9, 18*). Prior to the reactive transport simulations, groundwater flow was simulated with MODFLOW (*19*). The dimension of the modeled transect (40 m) was selected such that the model would capture the plume evolution between the source zone and the multilevel well. In the vertical direction, the model domain extended between 22 m asl (above sea level; bottom of aquifer) and 34 m asl (i.e., above the groundwater table). Groundwater flow at the site was generally unsteady, exhibiting small interannual water table fluctuations of mostly <40 cm. However, around the time for which the model was set up and calibrated, the time-scale of the transport between source zone and the monitoring well (∼8 days) was smaller than the time-scale of significant water table changes. For this study it was therefore assumed that the flow field and the contaminant plumes were approximately at steady state. The reactive transport model was run for a spin-up period until microbial lag times were overcome and steady state concentrations were established throughout the model domain for all aqueous species. Further details on the model discretization and the flow model setup are provided in the SI.

Overview of the Reaction Network. A conceptual model for the reactive processes was developed by qualitatively interpreting the measured hydrogeochemical data and translating it into a numerical model by formulating a reaction network of mixed equilibrium and kinetically controlled homogeneous and heterogeneous reactions. This site-specific reaction network was then implemented into the simulator's reaction database. The final version of the reaction network contained (i) all major ions, (ii) a limited number of minerals/mineral reactions potentially affecting aqueous concentrations, (iii) all major dissolved organic contaminants found at the site (iv), the corresponding immobile NAPL compounds and (v) biomass consisting of sulfate-reducing bacteria. The organic compounds included in the reaction network were benzene, toluene, ethylbenzene, *o*-xylene, *m*/*p*-xylene, naphthalene, acenaphthene, and fluorene. Among these, toluene is generally seen to be the most readily oxidizable compound (*20, 21*), followed by the other monoaromatic hydrocarbons and naphthalene, whereas acenaphthene and fluorene are considered to degrade slowly or potentially to be recalcitrant under sulfate reducing conditions (*22, 23*). For each organic compound two separate species were defined (e.g., refs *9, 18, and 24)*, one representing the lighter carbon pool (^{12}C) and one describing the heavier fraction (^{13}C). Similarly, redox states of sulfur, S(VI) and S(-II), were separated into a heavier (^{34}S) and a lighter (^{32}S) fraction. The equilibrated aqueous solution representing the ambient water composition is given in Table 1.

TABLE 1. Initial (Ambient) and Upgradient Boundary Water Composition in the Model Simulations, Corresponding to Measured Values from an Upgradient Infiltration Well

aqueous component	concentration [mol L^{-1}][b]
O(0)[a]	0
Ca	4.629×10^{-3}
Mg	7.748×10^{-4}
Na	2.488×10^{-3}
K	2.943×10^{-4}
Fe(2)[a]	5.871×10^{-10}
Fe(3)[a]	0
Cl	3.007×10^{-3}
C(4)[a]	6.652×10^{-3}
N	1×10^{-4}
pH	7.288
pe	−4.007
sulfate (light)	2.192×10^{-3}
sulfate (heavy)	1.021×10^{-4}
sulfide (light)	0
sulfide (heavy)	0

[a] Values in parentheses indicate valence. [b] Except pH and pe at bottom of the table.

Reaction Kinetics of Microbially Mediated Degradation Reactions. Previous investigations at the study site have identified microbially mediated sulfate reduction as the key process that is generally predominantly responsible for the mineralization of aromatic hydrocarbons and for the secondary geochemical changes triggered by the primary biodegradation reactions (*11, 25, 26*). For example, molecular analysis of the microbial community identified sulfate reducers (i.e., *Desulfocapsa* and *Desulfosporosinus*) as dominant microorganisms in the aquifer (*25*). These studies also found that >97% of the microbial community is attached to the sediments. In the numerical model, microbial activity was represented by a consortium of sediment-bound sulfate reducing bacteria (SRB). Concentrations of SRB were assumed to be affected by growth and decay, as discussed in, for example, Prommer et al. (*17, 27*):

$$\frac{\partial X}{\partial t} = \left.\frac{\partial X}{\partial t}\right|_{\text{growth}} + \left.\frac{\partial X}{\partial t}\right|_{\text{decay}} \quad (1)$$

where X is the concentration of the SRB. Microbial growth, which quantifies the rate at which organic carbon from n_{org} different organic compounds (i.e., from the various aromatic hydrocarbons) is converted to cell material, was modeled as

$$\left.\frac{\partial X}{\partial t}\right|_{\text{growth}} = \sum_{i=1,n_{\text{org}}} \upsilon_{\max,i} Y_{X,i} \frac{C_{\text{Org},i}}{K_{\text{Org},i} + C_{\text{Org},i}} \frac{C_{\text{Sulf}}}{K_{\text{Sulf}} + C_{\text{Sulf}}} X \quad (2)$$

where υ_{max} is the maximum microbial uptake rate, C_{org} is the concentration of the hydrocarbon compound, C_{sulf} is the sulfate concentration, K_{org}, and K_{sulf} are the appropriate half-saturation constants and Y_x is a stoichiometric factor expressing microbial yield. Many factors may influence

TABLE 2. Model Parameters Used to Simulate Biodegradation of BTEX and PAHs under the Prevailing Sulfate Reducing Conditions

compound	microbial uptake rate constant (mol L^{-1})	estimated molar fraction $\gamma_{org,i}$	Initial stable isotope ratio ($\delta^{13}C$, $\delta^{34}S$)	enrichment factor ϵ (reference)
benzene	2.5×10^{-5}	0.00006		
toluene	5×10^{-4}	0.155	−25.0	−2[a]
ethylbenzene	1×10^{-4}	0.0225	−24.9	−3.7(*33*)
m/*p*-xylene	7.5×10^{-5}	0.21	−24.5	−1.8(*32*)
o-xylene	1×10^{-4}	0.1	−24.8	−3.2(*33*)
naphthalene	1×10^{-4}	0.4	−24.5	−1.1(*29*)
acenaphthene	0	0.08235		
fluorene	0	0.11		
sulfate	na[c]	na	20	−13[b]

[a] Intermediate value of enrichment factors (sulfate reducing conditions) as described in ref *30*. [b] Intermediate value of enrichment factors derived from organic-rich aquifers as reported in refs *35 and 36*. [c] na stands for not available.

bacterial decay, including protozoan grazing, contaminant toxicity, and lack of nutrients. However, little quantitative information is available to describe these effects on microbial decay, in particular under in situ conditions. Therefore, the decay term was described using the standard assumption of a linear dependence on the biomass concentration:

$$\left.\frac{\partial X}{\partial t}\right|_{\text{decay}} = -k_{\text{dec}}X \tag{3}$$

where k_{dec} is a decay rate constant.

The removal rate of the i^{th} organic compound was proportional to the microbial growth rate:

$$\frac{\partial C_{\text{Org},i}}{\partial t} = \upsilon_{\text{max},i} Y_{\text{Org},i} \frac{C_{\text{Org},i}}{K_{\text{Org},i} + C_{\text{Org},i}} \frac{C_{\text{Sulf}}}{K_{\text{Sulf}} + C_{\text{Sulf}}} X \tag{4}$$

The stoichiometric factor $Y_{\text{Org},i}$ can be determined from the balanced degradation reactions that incorporate growth and thus a partial incorporation of the (degraded) organic carbon into cell mass. A microbial efficiency of 10% was assumed for sulfate reduction (*28*). For example, the reaction stoichiometry for toluene degradation under sulfate-reducing condition is then

$$C_7H_8 + 0.14NH_4^+ + 4.15SO_4^{2-} + 2.58H_2O + 1.86H^+ \rightarrow \rightarrow 6.3HCO_3^- + 0.14C_5H_7O_2N + 4.15H_2S \tag{5}$$

where $C_5H_7O_2N$ is the nominal molecular formula for the microbes. Thus, the stoichiometric factor Y_{Toluene} yields 0.14 (see SI Table SI-2 for all other reactions).

Carbon Isotope Fractionation. While the use of stable isotope signatures as indicators of microbially mediated removal of aromatic hydrocarbons has become a standard tool (*29*−*31*), multidimensional numerical modeling studies that included isotope fractionation processes associated with a complex set of biogeochemical reactions were not yet reported for field-scale problems. Molecules containing the heavier isotope ^{13}C degrade at relatively slower rates than those composed exclusively of the more abundant light isotope ^{12}C (*22*). This results in a successively increasing isotopic ratio, $\delta^{13}C$, of the residual contaminant during biodegradation. To consider this effect in the numerical model, separate light and heavy fractions were included in the reaction network for each dissolved organic compound (*9, 18, 24*). Therefore, the concentrations of both the lighter and heavier fractions could be tracked individually and the spatial distribution of the isotopic ratios could be computed subsequently from the simulated concentrations of the two fractions. In our model we assumed two different microbial uptake rates for the lighter and heavier fraction, respectively. While the uptake rate of the lighter isotopes was computed after eq 4, the uptake of the heavier isotopes was calculated from

$$\frac{\partial {}^{13}C_{\text{Org},i}}{\partial t} = \frac{\partial C_{\text{org},i}}{\partial t} \frac{{}^{13}C_{\text{org},i}}{{}^{12}C_{\text{org},i}} \alpha_{\text{Org},i} \tag{6}$$

where $\alpha_{\text{Org},i}$ represents the kinetic isotope fractionation factor, which equals the ratio of the two reaction rates. It can be determined from the enrichment factor ϵ:

$$\alpha_{\text{Org},i} = \varepsilon + 1 \tag{7}$$

All ϵ values used in this study (see Table 2) were adopted from values reported in the literature. Under sulfate-reducing conditions, values for ϵ range between −1.8 and −3.7‰ for monoaromatic hydrocarbons (*30, 32, 33*), whereas for naphthalene ϵ was assumed to be −1.1‰ (*29*).

Sulfate Reduction and Sulfur Isotope Fractionation. As for carbon isotope fractionation, the preferential conversion of isotopically lighter sulfate during microbial reduction causes an enrichment of the heavier ^{34}S in the residual sulfate pool (*34*). The differential consumption of ^{32}S and ^{34}S sulfate pools is governed by

$$\frac{\partial {}^{34}SO_4^{-2}}{\partial t} = \frac{\partial SO_4^{-2}}{\partial t} \frac{{}^{34}SO_4^{-2}}{{}^{32}SO_4^{-2}} \alpha_{SO_4^{-2}} \tag{8}$$

with $\alpha_{SO_4^{-2}}$ representing the kinetic isotope fractionation factor for sulfate reduction. The consumption of sulfate as electron acceptor during hydrocarbon mineralization was computed from:

$$\frac{\partial SO_4^{-2}}{\partial t} = \sum_{i=1,n_{\text{org}}} \frac{\partial C_{\text{org},i}}{\partial t} Y_{SO_4^{-2},i} \tag{9}$$

where the stoichiometric factor $Y_{SO_4^{-2},i}$ links the degradation rates of individual hydrocarbon compounds with the corresponding sulfate consumption rates. The overall sulfate reduction rate is governed by the sum of the n_{org} consumption rates. Following previous reports of enrichment factors from field studies (*35, 36*), a mean ϵ value of −13‰ was used for sulfate isotope fractionation. Measured concentrations of dissolved sulfide were very low, thus suggesting that reduced sulfur was quickly precipitating as FeS or pyrite. Since the measured dissolved iron concentrations in the ambient water (2.0×10^{-7}mol L^{-1}) as well as in the plume core (<5×10^{-6} mol L^{-1}) were far below the required amount for stoichiometric FeS or pyrite precipitation, dissolution of goethite was assumed to be acting as primary source of iron in the model. Such a reaction between ferric iron and biogenic sulfide has been reported earlier by Beller et al. (*28*) for a case of toluene degradation under sulfate-reducing conditions.

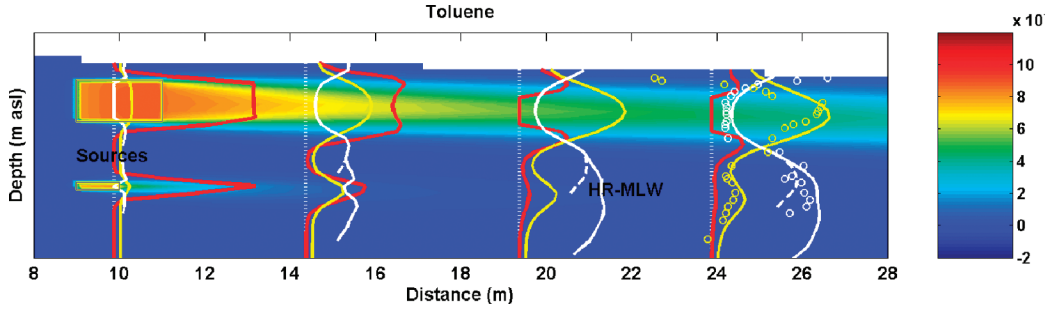

FIGURE 1. Simulated concentration contours of toluene and selected depth profiles of simulated toluene degradation rates (solid red lines) in comparison with the simulated carbon isotope signature of toluene (solid white lines) and sulfur isotope signature (solid yellow lines). Circles indicate corresponding values measured at the high-resolution multilevel well. The dashed white lines show the carbon isotope signature resulting from the simulation in which the lower source zone was deactivated.

Contaminant Source Geometry, Source Composition and Dissolution Kinetics. The measurements of dissolved contaminant concentrations and biogeochemical parameters indicated the presence of two distinct contamination sources. Therefore, in the numerical model, two NAPL source zones located 15 m upstream of the multilevel well were assumed to continuously release BTEX and PAH constituents. The thickness of the upper source zone was assumed to be 0.3 m. The lower zone, which was quantitatively less significant and presumably consisted of entrapped NAPL residuals (*37*), was only 0.05 m thick. The kinetically controlled dissolution rate for each compound from these source zones was computed from ref *27*:

$$\frac{-\partial C_{org,napl}}{\partial t} = \varpi(C_{org,aqu} - C_{org,mc}) \quad (10)$$

where $C_{org,napl}$ and $C_{org,\ aqu}$ are the immobile (NAPL) and the aqueous concentration of the hydrocarbon compound, respectively, $C_{org,mc}$ is the multicomponent solubility and ϖ is a rate transfer constant. Following Raoult's law, $C_{org,mc}$ in eq 10 can be computed from the known single-species solubility of the hydrocarbon compound and its mole fraction γ_{org} in the NAPL mixture:

$$C_{org,mc} = \gamma_{org} C_{org,solub} \quad (11)$$

However, in the present study the NAPL composition and the molar fractions γ_{org} were unknown and had to be estimated during the model calibration (see Table 2).

Model Calibration Strategy. The selected reaction network contains a significant number of a priori unknown, adjustable parameters, such as reaction rate constants, that needed to be determined as part of the model calibration. Moreover, the uncertainty of the exact source dimensions and source composition was a significant challenge for constraining the model simulations rigorously. However, on the other hand there were also a large number of observations (detailed concentration and isotope measurements) which, together with specific, simplifying assumptions, eventually provided sufficient constraints for the estimation of model parameters. Such simplifying assumptions were, for example, that the hydraulic conductivity within the domain was constant and well enough known from previous investigations. With these initial (reasonable) assumptions, the flow model was not further varied during the model calibration. The transverse dispersivity (α_T) was initially set to a typical value (1 mm) and then varied further during the model calibration. While none of the simulated compounds could be clearly identified and used as a (nonreactive) tracer in the calibration, the range of possible dispersivity values was still successfully bracketed during the calibration of the least reactive PAH compounds. With respect to the NAPL source, two important assumptions were that (i) the composition of the NAPL mixture was similar in all grid cells that were assumed to contain NAPLs and (ii) that NAPL dissolution was relatively fast and the corresponding high value for the rate transfer constant ϖ was essentially creating equilibrium dissolution conditions. Parameters controlling contaminant degradation were estimated by initially focusing the calibration on the most prominent degradable compounds with the highest electron acceptor (i.e., sulfate) consumption. The comparison of the simulated and measured sulfate concentration profiles, pH profiles and the measured $\delta^{34}S$ profiles served as key constraints for the lumped rate of organic contaminant oxidation. Rates of individual compounds were mainly adjusted by simultaneously fitting the observed concentration and $\delta^{13}C$ profiles. Throughout the model development and calibration process a range of alternative conceptual models was evaluated (see SI).

Results and Discussion

Simulated Fate of BTEX and PAH. In the model simulations, uncontaminated sulfate-containing groundwater passed through the NAPL source zones, where, for each of the simulated organic compounds, mass was transferred to the aqueous phase. At locations where both sulfate and aromatic hydrocarbons were simultaneously present, microbial growth occurred, thereby degrading the various hydrocarbons at compound-specific and spatially varying rates. Figure 1 shows the simulated steady-state toluene concentration contours and selected depth profiles of the simulated toluene degradation rates. These depth profiles suggest that near the source zone degradation occurred across the whole NAPL contaminated zone. However, further downgradient, biodegradation became most pronounced at the plume fringe due to the lack of sulfate in the plume core (Figure 2). At these locations mixing by transverse dispersion (calibrated $\alpha_T = 0.5$ mm) allows the degradation to proceed further. Figure 3 shows a detailed comparison of simulated hydrocarbon concentration profiles with the concentrations measured at the well. The plots also show the results from the corresponding (nonreactive) simulations, in which NAPL dissolution could occur but all biodegradation processes were switched off. For all hydrocarbon compounds considered, model simulations agreed favorably with the measured data. The only noteworthy discrepancy is the slight overestimation of *m*/*p*-xylene concentrations in the lower part of the profile, which corresponds to the lower source zone. Substantial differences between simulated reactive and nonreactive concentration profiles at the monitoring well existed mainly for toluene and ethylbenzene, whereas the other concentration profiles were less clearly affected by biodegradation. Note that in the absence of better information, the simplifying assumption was made that the NAPL mixture (mole fractions) was similar in both source zones. In reality, mixtures and thus multicomponent solubilities may differ in space as a result of the spatially varying source depletion rates of the

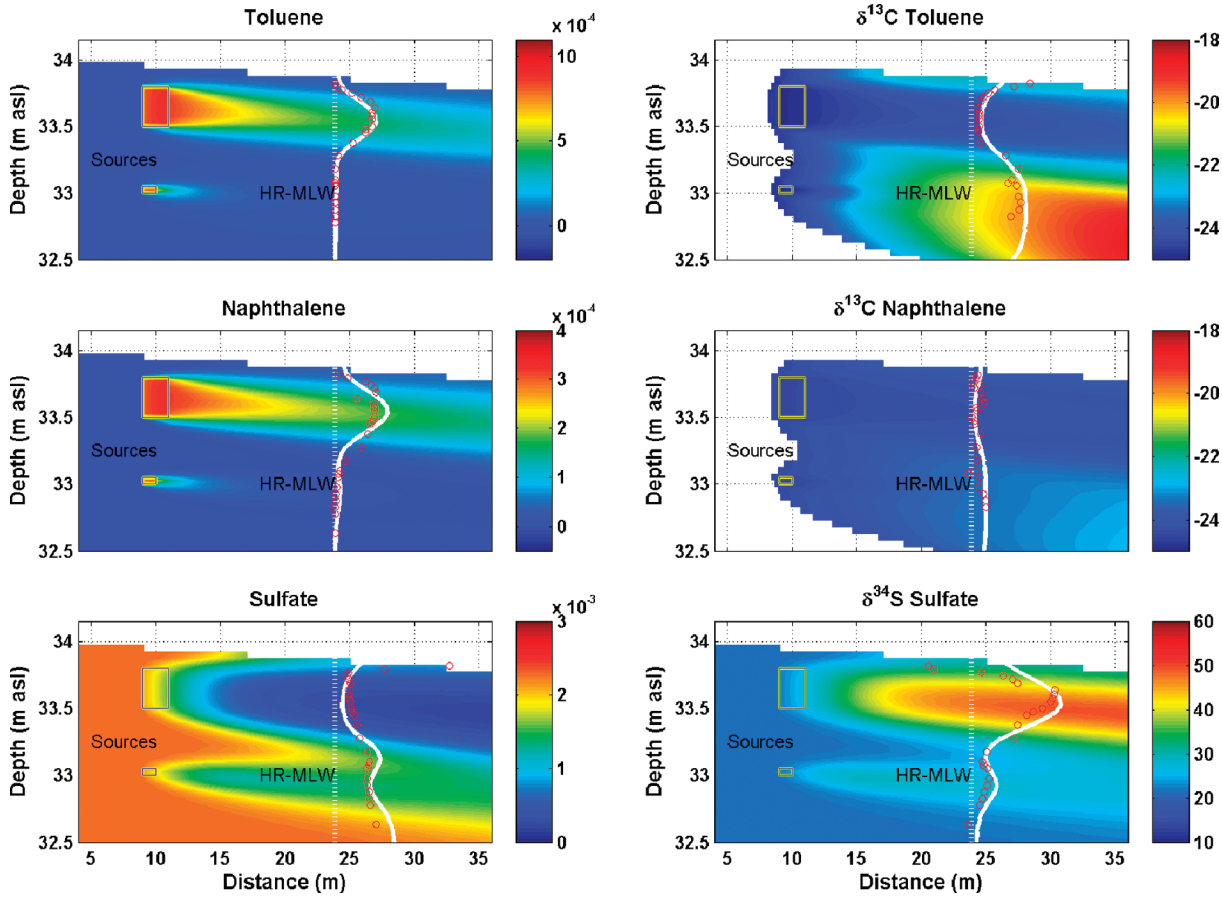

FIGURE 2. Simulated concentration contours of toluene, naphthalene, sulfate and associated isotope signatures. Solid white lines indicate simulated and red circles indicate measured values at the high-resolution well.

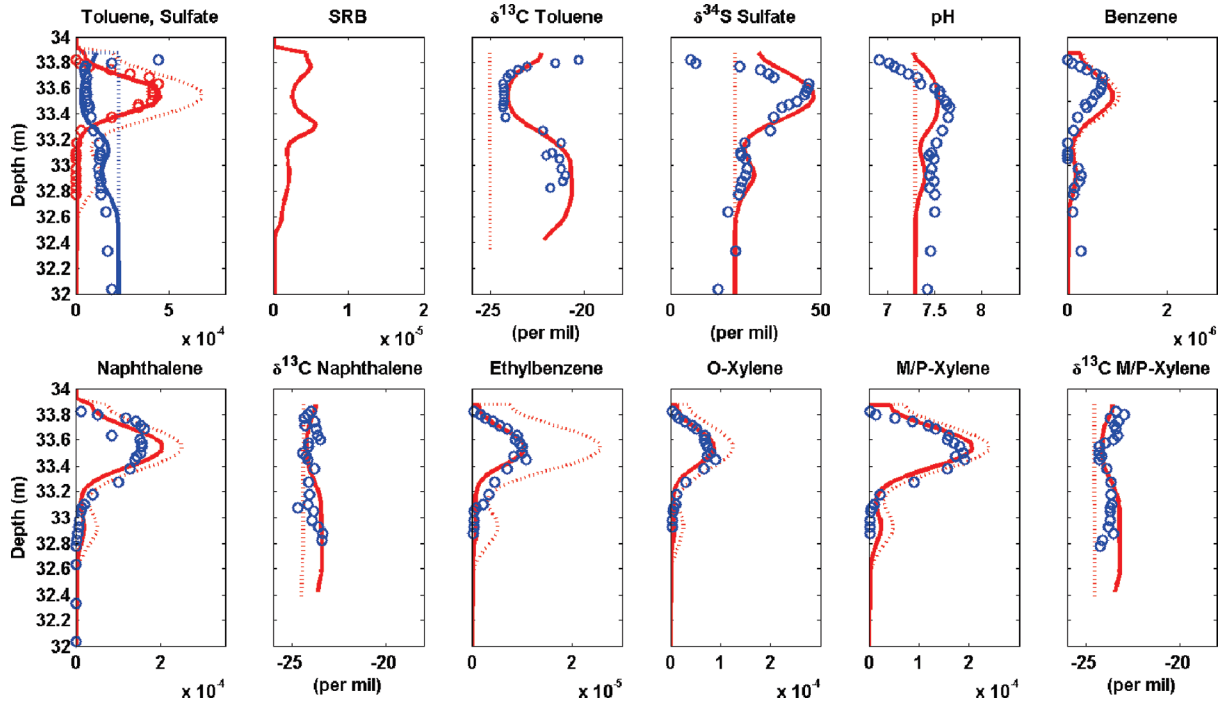

FIGURE 3. Selected simulated (reactive and nonreactive: solid and dot lines, respectively) and measured concentration (circles) depth profiles and associated isotopic signatures at the multilevel well. All concentrations, including microbial concentrations, are given in mol L^{-1}.

various compounds. The degradation behavior that can be inferred from the model-based interpretation agrees with literature reports that anaerobic oxidation of toluene proceeds appreciably faster compared to other aromatic hydrocarbons (see SI Table SI-4). In the calibrated model the computed toluene mass flux reduction between the source zone and

the multilevel well was 53% (naphtalene 32%, *m*/*p*-xylene 15%, *o*-xylene 26%, ethylbenzene 46%, benzene 69%) and accounted for 56% of the oxidation capacity (naphthalene 18%, *m*/*p*-xylene 12%, *o*-xylene 10%, ethylbenzene 3%, benzene 0.02%, see also SI Figure SI-2).

Simulated Carbon Isotope Signatures. Measurements and simulation results exhibit clear variations in the carbon isotope enrichment and distinct spatial variations. These were most pronounced for the most degradable compound toluene while being less clear for the more slowly degradable compounds. Similar to the measured data, the simulations for toluene showed significant differences in the isotopic enrichment between the plume center (≤0.5‰) and the plume fringes (see Figures 2 and 3 for comparison). At the lower plume fringe, an enrichment of up to 3.3‰ was measured at the multilevel well, which was accurately reproduced by the model. Figure 1 shows the evolution of the simulated carbon isotope ratios between the source zones and the groundwater well via selected depth profiles, whereas Figure 2 shows contour plots of both simulated concentrations as well as the corresponding isotope ratios. In the present case the smaller carbon isotope enrichment for toluene in the plume core results from a combination of factors. First, a significant part of the toluene mass removal occurred in the source zone itself, where degradation triggered additional dissolution of toluene that had the initial (nonenriched) carbon isotope ratio. Second, further downgradient of the source zone, degradation proceeded solely at the plume fringes, as discussed before and as indicated by the degradation rate depth profiles shown in Figure 1. We also investigated to what extent the plume originating from the lower source, which was degraded more completely, affected the carbon isotope profile. While these comparative simulations without the lower source zone indicated some influence on the lower part of the carbon isotope profiles, including the high-resolution well location, the lower source was not responsible for the strong gradients (Figure 1).

In contrast to toluene, only slight changes in the isotope signatures were observed for the more slowly degrading *m*/*p*-xylene and for naphthalene, where the higher number of C atoms in the molecule is additionally responsible for the moderate isotope fractionation (Figure 3). Measured benzene concentrations were below the detection limit of the CSIA-method, thus isotope ratios were not determined.

Simulated Sulfate Reduction and Sulfate Isotope Signatures. While groundwater passed through the upper NAPL source zone, oxidation of hydrocarbon compounds consumed most of the sulfate for which the background water concentration was 2.3×10^{-3} mol L^{-1}. Downstream of the upper NAPL source zone, sulfate remained at low concentrations throughout the core of the plume. As shown in Figure 3, the profile of the sulfur isotope signature at the multilevel well exhibits an enrichment of up to 30‰. In contrast to the toluene carbon isotopes, which showed a maximum enrichment outside the plume, the maximum ^{34}S enrichment occurred in the center of the upper contaminant plume. In the plume core, where most of the sulfate was degraded, the sulfate pool remained enriched in the heavier ^{34}S isotope, whereas at the plume fringe, transverse dispersion leads to a dilution of the enriched isotope signature.

In the lower, presumably much smaller source zone, sulfate was only partially consumed by the hydrocarbons released from the NAPL. Given the numerous simplifying assumptions made for the source definition (geometry, mass-transfer rates, contaminant mixture), the modeled sulfate concentration profiles as well as the associated sulfur isotope signature (Figure 3) agreed very well with the data collected from the high-resolution well. As Figure 3 shows, modeled $\delta^{34}S$-values just below the groundwater table overestimated the measured values, which decreased to 6.6‰ in this zone, i.e., to values below the $\delta^{34}S$ value that were assumed to represent ambient conditions. The lower values could possibly point to the reoxidation of previously precipitated iron sulfides when oxidants can access the sulfides during water table fluctuations. However, as we assumed steady state flow, these oxidation processes could not be represented in the current model. The reoxidation of iron sulfides could also explain the pronounced decrease of the measured pH toward the groundwater table, where it dropped to below the ambient values found deeper in the saturated zone. At this location the simulated pH overestimates the measured values, whereas it is in good agreement elsewhere.

Acknowledgments

We thank Peter Franzmann and Colin Johnston for their helpful comments on earlier versions of this manuscript, Greg Davis for discussions and Martin Elsner for his assistance with isotope measurements. We are also thankful for the assistance of Lars Richters and Paul Eckert (Stadtwerke Düsseldorf). The support of the DFG project FOR 525/1 "Reactions in Porous Media", IVEC Western Australia for HPC support and Schlumberger Water Services for GUI software support is gratefully acknowledged.

Note Added after ASAP Publication

There were minor changes made to Table 1, equations 6 and 8, and the last paragraph of the Results and Discussion section, in the version of this paper published ASAP September 24, 2009; the corrected version published ASAP October 2, 2009.

Supporting Information Available

Additional information on the study site and the setup and definition of the numerical model. This material is available free of charge via the Internet at http://pubs.acs.org.

Literature Cited

(1) Cirpka, O. A.; Frind, E. O.; Helmig, R. Numerical simulation of biodegradation controlled by transverse mixing. *J Contam Hydrol* **1999**, *40*, 159–182.
(2) Bauer, R. D.; Maloszewski, P.; Zhang, Y.; Meckenstock, R. U.; Griebler, C. Mixing-controlled biodegradation in a toluene plume - Results from two-dimensional laboratory experiments. *J Contam Hydrol* **2008**, *96*, 150–168.
(3) Bauer, R. D.; Rolle, M.; Bauer, S.; Eberhardt, C.; Grathwohl, P.; Kolditz, O.; Meckenstock, R. U.; Griebler, C. Enhanced biodegradation by hydraulic heterogeneities in petroleum hydrocarbon plumes. *J Contam Hydrol* **2009**, *105*, 56–68.
(4) Bauer, R. D.; Rolle, M.; Kürzinger, P.; Grathwohl, P.; Meckenstock, R. U.; Griebler, C. Two-dimensional flow-through microcosms: versatile test systems to study biodegradation processes in porous aquifers. *J. Hydrol.* **2009**, *369*, 284–295.
(5) Rees, H. C.; Oswald, S. E.; Banwart, S. A.; Pickup, R. W.; Lerner, D. N. Biodegradation processes in a laboratory-scale groundwater contaminant plume assessed by fluorescence imaging and microbial analysis. *Appl. Environ. Microbiol.* **2007**, *73*, 3865–3876.
(6) Davis, G. B.; Barber, C.; Power, T. R.; Thierrin, J.; Patterson, B. M.; Rayner, J. L.; Quinglong, W. The variability and intrinsic remediation of a BTEX plume in anaerobic sulphate-rich groundwater. *J. Contam. Hydrol.* **1999**, *36*, 265–290.
(7) Tuxen, N.; Albrechtsen, H. J.; Bjerg, P. L. Identification of a reactive degradation zone at a landfill leachate plume fringe using high resolution sampling and incubation techniques. *J. Contam. Hydrol.* **2006**, *85*, 179–194.
(8) van Breukelen, B. M.; Griffioen, J. Biogeochemical processes at the fringe of a landfill leachate pollution plume: potential for dissolved organic carbon, Fe(II), Mn(II), NH_4^+, and CH_4 oxidation. *J. Contam. Hydrol.* **2004**, *73*, 181–205.
(9) van Breukelen, B. M.; Prommer, H. Beyond the Rayleigh equation: reactive transport modeling of isotope fractionation effects to improve quantification of biodegradation. *Environ. Sci. Technol.* **2008**, *42*, 2457–63.

(10) Fischer, A.; Theuerkorn, K.; Stelzer, N.; Gehre, M.; Thullner, M.; Richnow, H. H. Applicability of stable isotope fractionation analysis for the characterization of benzene biodegradation in a BTEX-contaminated aquifer. *Environ. Sci. Technol.* **2007**, *41*, 3689–3696.
(11) Anneser, B.; Einsiedl, F.; Meckenstock, R. U.; Richters, L.; Wisotzky, F.; Griebler, C. High-resolution monitoring of biogeochemical gradients in a tar oil-contaminated aquifer. *Appl. Geochem.* **2008**, *23*, 1715–1730.
(12) Anneser, B.; Richters, L.; Griebler, C., Application of high-resolution groundwater sampling in a tar oil—contaminated sandy aquifer. Studies on small-scale abiotic gradients. In *Advances in Subsurface Pollution of Porous Media: Indicators, Processes and Modelling*; Candela, L., Vadillo, I., Elorza, F. J., Eds.; CRC Press/Balkema: Leiden, NL, 2008; pp 107—122.
(13) Zwank, L.; Berg, M.; Schmidt, T. C.; Haderlein, S. B. Compound-specific carbon isotope analysis of volatile organic compounds in the low-microgram per liter range. *Anal. Chem.* **2003**, *75*, 5575–83.
(14) Prommer, H.; Barry, D. A.; Zheng, C. MODFLOW/MT3DMS-based reactive multicomponent transport modeling. *Ground Water* **2003**, *41*, 247–257.
(15) Greskowiak, J.; Prommer, H.; Massmann, G.; Nützmann, G. Modeling seasonal redox dynamics and the corresponding fate of the pharmaceutical residue phenazone during artificial recharge of groundwater. *Environ. Sci. Technol.* **2006**, *40*, 6615–6621.
(16) Prommer, H.; Grassi, M. E.; Davis, A. C.; Patterson, B. M. Modeling of microbial dynamics and geochemical changes in a metal bioprecipitation experiment. *Environ. Sci. Technol.* **2007**, *41*, 8433–8438.
(17) Prommer, H.; Tuxen, N.; Bjerg, P. L. Fringe-controlled natural attenuation of phenoxy acids in a landfill plume: integration of field-scale processes by reactive transport modeling. *Environ. Sci. Technol.* **2006**, *40*, 4732–8.
(18) Prommer, H.; Aziz, L. H.; Bolaño, N.; Taubald, H.; Schüth, C. Modelling of geochemical and isotopic changes in a column experiment for degradation of TCE by zero-valent iron. *J. Contam. Hydrol.* **2008**, *97*, 13–26.
(19) McDonald, J. M.; Harbaugh, A. W. *MODFLOW. A Modular 3D Finite Difference Ground Water Flow Model*, Open file report; U.S. Geological Survey: Reston, VA, 1988; pp 83—875.
(20) Edwards, E. A.; Wills, L. E.; Reinhard, M.; Grbic-Galic, D. Anaerobic degradation of toluene and xylene by aquifer microorganisms under sulfate-reducing conditions. *Appl. Environ. Microbiol.* **1992**, *58*, 794–800.
(21) Thierrin, J.; Davis, G. B.; Barber, C.; Patterson, B. M.; Pribac, F.; Power, T. R.; Lambert, M. Natural degradation rates of BTEX compounds and naphthalene in a sulphate reducing groundwater environment. *Hydrol. Sci J.* **1993**, *38*, 309–322.
(22) Meckenstock, R.; Safinowski, M.; Griebler, C. Anaerobic degradation of polycyclic aromatic hydrocarbons. *FEMS Microbiol. Ecol.* **2004**, *49*, 27–36.
(23) Spormann, A. M.; Widdel, F. Metabolism of alkylbenzenes, alkanes, and other hydrocarbons in anaerobic bacteria. *Biodegradation* **2000**, *11*, 85–105.
(24) van Breukelen, B. M.; Hunkeler, D.; Volkering, F. Quantification of sequential chlorinated ethene degradation by use of a reactive transport model incorporating isotope fractionation. *Environ. Sci. Technol.* **2005**, *39*, 4189–4197.
(25) Winderl, C.; Anneser, B.; Griebler, C.; Meckenstock, R. U.; Lueders, T. Depth-resolved quantification of anaerobic toluene degraders and aquifer microbial community patterns in distinct redox zones of a tar oil contaminant plume. *Appl. Environ. Microbiol.* **2008**, *74*, 792–801.
(26) Wisotzky, F.; Eckert, P. Sulfat-dominierter BTEX-Abbau im Grundwasser eines ehemaligen Gaswerksstandortes. *Grundwasser* **1997**, *2*, 11–20.
(27) Prommer, H.; Barry, D. A.; Davis, G. B. Modelling of physical and reactive processes during biodegradation of a hydrocarbon plume under transient groundwater flow conditions. *J. Contam. Hydrol.* **2002**, *59*, 113–131.
(28) Beller, H. R.; Grbic-Galic, D.; Reinhard, M. Microbial degradation of toluene under sulfate-reducing conditions and the influence of iron on the process. *Appl. Environ. Microbiol.* **1992**, *58*, 786–93.
(29) Griebler, C.; Safinowski, M.; Vieth, A.; Richnow, H. H.; Meckenstock, R. U. Combined application of stable carbon isotope analysis and specific metabolites determination for assessing *in situ* degradation of aromatic hydrocarbons in a tar oil-contaminated aquifer. *Environ. Sci. Technol.* **2004**, *38*, 617–31.
(30) Meckenstock, R. U.; Morasch, B.; Griebler, C.; Richnow, H. H. Stable isotope fractionation analysis as a tool to monitor biodegradation in contaminated aquifers. *J. Contam. Hydrol.* **2004**, *75*, 215–55.
(31) Richnow, H. H.; Meckenstock, R. U.; Reitzel, L. A.; Baun, A.; Ledin, A.; Christensen, T. H. *In situ* biodegradation determined by carbon isotope fractionation of aromatic hydrocarbons in an anaerobic landfill leachate plume (Vejen, Denmark). *J. Contam. Hydrol.* **2003**, *64*, 59–72.
(32) Morasch, B.; Richnow, H. H.; Vieth, A.; Schink, B.; Meckenstock, R. U. Stable isotope fractionation caused by glycyl radical enzymes during bacterial degradation of aromatic compounds. *Appl. Environ. Microbiol.* **2004**, *70*, 2935–40.
(33) Wilkes, H.; Boreham, C.; Harns, G.; Zengler, K.; Rabus, R. Anaerobic degradation and carbon isotopic fractionation of alkylbenzenes in crude oil by sulphate-reducing bacteria. *Org. Geochem.* **2000**, *31*, 101–115.
(34) Einsiedl, F.; Mayer, B. Sources and processes affecting sulfate in a karstic groundwater system of the Franconian Alb, southern Germany. *Environ. Sci. Technol.* **2005**, *39*, 7118–25.
(35) Bottrell, S. H.; Hyes, P. J.; Bannon, M.; Williams, G. M. Bacterial sulfate reduction and pyrite formation in a polluted sand aquifer. *Geomicrobiol. J.* **1995**, *13*, 75–90.
(36) Spence, M. J.; Bottrell, S. H.; Thornton, S. F.; Richnow, H. H.; Spence, K. H. Hydrochemical and isotopic effects associated with petroleum fuel biodegradation pathways in a chalk aquifer. *J. Contam. Hydrol.* **2005**, *79*, 67–88.
(37) Eckert, P.; Appelo, C. A. J. Hydrogeochemical modeling of enhanced benzene, toluene, ethylbenzene, xylene (BTEX) remediation with nitrate. *Water Resour. Res.* **2002**, *38*, 1–11.

ES901142A